PERGAMON

International Journal of Heat and Mass Transfer 46 (2003) 871–877

International Journal of HEAT and MASS TRANSFER

www.elsevier.com/locate/ijhmt

Performance of finned tube heat exchangers operating under frosting conditions

Wei-Mon Yan [a,*], Hung-Yi Li [a], Yeun-Jong Wu [b], Jian-Yuan Lin [c], Wen-Ruey Chang [c]

[a] *Department of Mechanical Engineering, Huafan University, Shihtin, Taipei 22305, Taiwan, ROC*

[b] *Graduate Institute of Mechatronic Engineering, Huafan University, Shihtin, Taipei 22305, Taiwan, ROC*

[c] *Energy and Resources Laboratories, Industrial Technology Research Institute, Chutung, Hsinchu 310, Taiwan, ROC*

Received 22 June 2002; received in revised form 8 July 2002

Abstract

In this paper, the performance of flat plate finned tube heat exchangers operating under frosting conditions was investigated experimentally. Heat exchangers of single and multiple tube row(s) were tested to show the effects of various parameters on heat transfer performance. The parameters include temperature and relative humidity of air, flow rate of air, refrigerant temperature, fin pitch, and row number. The time variations of heat transfer rate, overall heat transfer coefficient, and pressure drop of heat exchangers presented.

1. Introduction

Frost formation on heat transfer surfaces is a serious problem in low-temperature applications such as refrigerator-freezers, freezers, and heat pumps. When moist air flows across cold heat exchanger surfaces whose temperatures are lower than the freezing temperature, condensation and frost formation occur on the heat exchanger surfaces. The process involves both heat and mass transfer between the air and the surfaces. Many researchers have studied the effects of the frost on the performance of various heat exchangers.

Overall heat transfer coefficient and air side pressure drop are two important factors to evaluate the performance of heat exchangers. Niederer [1] performed experiments to investigate the frosting and defrosting effects on the heat transfer in heat exchangers. He found that frost accumulation on the coil surface reduced the air flow rate and the heat exchanger capacity. Heat exchangers having wider fin spacing were affected with a lesser degree than those having closer fin spacing under frosting conditions. Heat exchangers with variable fin spacing performed better when compared with heat exchangers having a constant fin spacing. Kondepudi and O'Neal [2] comprehensively discussed the effects of frost on fin efficiency, overall heat transfer coefficient, pressure drop, and surface roughness of extended surface heat exchangers. They suggested that more model be highly needed to determine effects of frost on fin performance. Kondepudi and O'Neal [3] experimentally studied performance of louvered finned tube heat exchangers under frosting conditions. They reported that frost growth, pressure drop, and energy transfer coefficient increase with air humidity, air velocity, and fin density. Kondepudi and O'Neal [4] also compared performance of finned tube heat exchangers with different fin configurations. It was found that the louvered fin type has the best thermal performance, followed by the wavy fin type and the flat fin. Senshu et al. [5] and Yasuda et al. [6] investigated performance of heat pumps under frosting conditions experimentally and theoretically. The speed of frost formation could be assumed constant when the air and the refrigerant conditions were specified and raising the refrigerant evaporation temperature could reduce the possibility of frosting. The heat transfer coefficient of the air was not significantly affected by frosting. Oskarsson et al. [7,8] presented

* Corresponding author. Tel.: +886-2-26632102x4038; fax: +886-2-2663-3847.

E-mail address: wmyan@huafan.hfu.edu.tw (W.-M. Yan).

0017-9310/03/$ - see front matter
PII: S0017-9310(02)00346-0

Nomenclature

A	area	T	temperature
C_p	specific heat	t	time
F	correction factor	U	overall heat transfer coefficient
i	enthalpy	ϕ	relative humidity
$\dot{m}$	mass flow rate	*Subscripts*	
N	row number	a	air
ΔP	pressure drop	i	inlet
Q	volume flow rate	o	outlet
$\dot{Q}$	heat transfer rate	r	refrigerant
S	fin pitch		

equations, correlations, and models for evaporators operating with dry, wet, and frosted surfaces. Rite and Crawford [9,10] investigated the effects of various parameters on frost formation and performance of a domestic refrigerator-freezer finned tube evaporator. They concluded the frosting rate increased for higher air humidity, temperature, flow rate and lower refrigerant temperature. UA value and air side pressure drop increased as frost forms on the evaporator coil for a constant air flow rate. Kondepudi and O'Neal [11,12] proposed a model to evaluate performance of finned tube heat exchangers under frosting conditions. The numerical results of frost growth rate, air side pressure drop, and heat transfer coefficient were compared with the experimental results. It was indicated that the predicted results underpredicted by 15–20%. Recently, Thomas et al. [13] and Chen et al. [14] investigated the frost characteristics on heat exchanger fins.

The purpose of this paper is to investigate the effects of frost formation on performance of flat plate finned tube heat exchangers having various parameters, including temperature and relative humidity of air, flow rate of air, refrigerant temperature, fin pitch, and row number.

2. Experimental apparatus

In this work, the experimental setup contains a psychrometric room, heat exchanger test section, wind tunnel, refrigerant system, and data acquisition system. The psychrometric room provides conditioned air of constant temperature and relative humidity in the range -10 °C to 45 ± 0.3 °C and 40% to $95\% \pm 3\%$, respectively. Conditioned air from the psychrometric room was drawn through the wind tunnel by a 2.24 kW centrifugal fan with an inverter. Flat plate finned tube heat exchangers of single and multiple tube row(s) with various fin pitches were used to investigate the effects of frost on performance of heat exchangers. The detailed geometrical parameters of the heat exchangers are shown in Table 1. The refrigerant in the tube used was ethylene glycol water solution. The inlet refrigerant temperature is controlled by means of a thermostat reservoir. The inlet and outlet temperatures of the refrigerant, and the inlet and outlet (dry-bulb and wet-bulb) temperatures of air were measured by pre-calibrated RTDs (Pt-100) which have an accuracy of 0.2 °C. The measurements of the dry-bulb and wet-bulb temperatures of air across the heat exchanger were based on ASHRAE 14.1 standard [15] with two psychrometric boxes. The air flow rate was measured by multiple nozzles based on the ASHRAE 41.2 standard [16]. Precision differential pressure transducers with 0.1 Pa resolution were used to detect the pressure drops across the heat exchanger and the multiple nozzles, respectively. The flow rate of air was maintained constant throughout each test by adjusting the speed of the centrifugal fan. The refrigerant flow rate was measured by a

Table 1
Fin geometries

No.	Pitch no.	Fin pitch (mm)	Outer diameter (mm)	Width (mm)	Height (mm)	Depth (mm)	Row no.	Area (m^2)
1	369	1.6	10.3	590	356	37.2	2	8.626
2	327	1.8	10.3	590	356	18.6	1	3.812
3	327	1.8	10.3	590	356	37.2	2	7.625
4	327	1.8	10.3	590	356	55.8	3	11.437
5	327	1.8	10.3	590	356	74.4	4	15.249
6	292	2.0	10.3	590	356	37.2	2	6.867

Tube material: copper, fin material: aluminum, horizontal tube pitch: 25.4 mm, vertical tube pitch: 19.05 mm, tube thickness: 0.35 mm, fin thickness: 0.115 mm.

Table 2
Baseline testing conditions

Parameter	Value
Inlet refrigerant temperature	−15 °C
Inlet air temperature	5 °C
Inlet air relative humidity	70%
Air flow rate	24 m^3/min
Refrigerant flow rate	4.17 l/min
Fin pitch	1.8 mm
Row number	2

calibrated magnetic flow meter with 0.002 L/s resolution. The data were recorded every five minutes with the acquisition system that transmitted the data to the personal computer for further operation. The baseline testing conditions for these parameters are shown in Table 2.

3. Data reduction

The variables measured were inlet and outlet air dry-bulb and wet-bulb temperatures of the heat exchanger, air flow rate, pressure drop of air across heat exchanger, inlet and outlet refrigerant temperatures, flow rate of refrigerant, and air pressure drop across the nozzles. The heat transfer rate and the overall heat transfer coefficient of the heat exchanger were obtained from the experimental data.

3.1. Heat transfer rate

Since frosting process includes both sensible and latent heat transfer for the air side, the heat transfer rate of the air side can be calculated by

$$\dot{Q}_a = \dot{m}_a(i_{a,i} - i_{a,o}) \tag{1}$$

where $\dot{Q}_a$ is the heat transfer rate, $\dot{m}_a$ is the mass flow rate, $i_{a,i}$ and $i_{a,o}$ are the enthalpies of air at inlet and outlet of the heat exchanger, respectively.

The heat transfer rate of the refrigerant side can be computed by

$$\dot{Q}_r = \dot{m}_r C_{p,r}(T_{r,o} - T_{r,i}) \tag{2}$$

where $\dot{Q}_r$ is the heat transfer rate, $\dot{m}_r$ is the mass flow rate, $C_{p,r}$ is the specific heat, $T_{a,i}$ and $T_{a,o}$ are the temperatures of the refrigerant at the inlet and outlet of the heat exchanger, respectively.

Before conducting the experiments, preliminary tests showed that the differences between $\dot{Q}_a$ and $\dot{Q}_r$ without frost formation are within 5%. Since there are difficulties to calculate $\dot{Q}_a$ for air with temperature below 0 °C, therefore, $\dot{Q}_r$ was adopted for the results presented in this paper.

Table 3
Summary of estimated uncertainties

Parameter	Uncertainty
Q_r	±0.002 l/s
ρ_r	±2 kg/m^3
T_r	±0.2 °C
T_a	±0.2 °C
ϕ	±3% RH
$\dot{Q}$	±6.83%
U	±7.63%
ΔP	±2.12%

3.2. Overall heat transfer coefficient

The overall heat transfer coefficient U can be expressed as

$$U = \frac{\dot{Q}}{A(\mathrm{LMTD})F} \tag{3}$$

where F is the correction factor, A is the frontal area without frosting, and the log-mean temperature difference (LMTD) is defined as

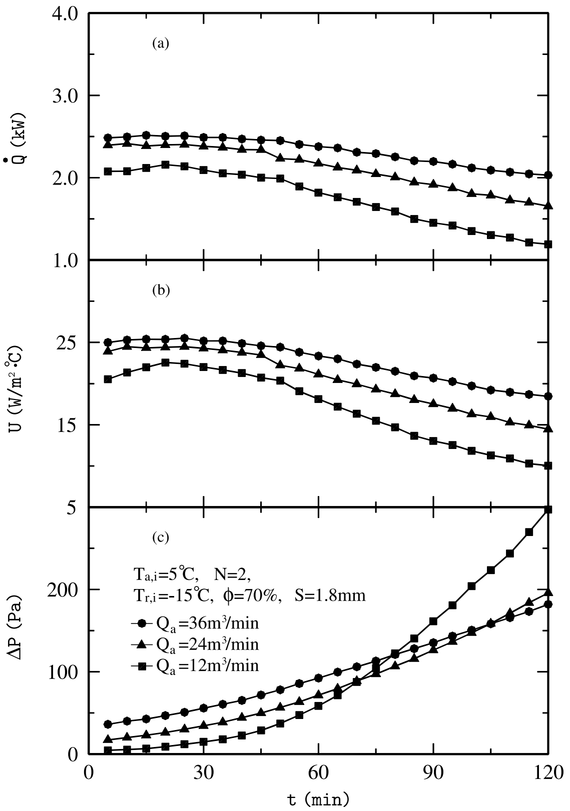

Fig. 1. Effects of air flow rate on (a) heat transfer rate, (b) overall heat transfer coefficient, and (c) pressure drop.

$$\mathrm{LMTD} = \frac{\Delta T_1 - \Delta T_2}{\ln\left(\frac{\Delta T_1}{\Delta T_2}\right)} \tag{4}$$

where

$$\Delta T_1 = T_{a,i} - T_{r,o} \tag{5}$$

$$\Delta T_2 = T_{a,o} - T_{r,i} \tag{6}$$

The uncertainties for the experimental results were calculated according to the procedure outlined by Kline and McClintock [17]. The results of the uncertainty analysis are tabulated in Table 3.

4. Results and discussion

The effects of air flow rate, air relative humidity, air temperature, refrigerant temperature, fin pitch, and row number on heat transfer rate, overall heat transfer coefficient, and air side pressure drop of heat exchangers operating under frosting conditions were investigated. The experiments were performed at the baseline conditions as listed in Table 2 except for the variable being evaluated. Fig. 1 shows the effects of air flow rate on heat transfer and pressure drop characteristics of heat exchanger. It is noted from Fig. 1(a) and (b) that a higher air flow rate leads to a higher heat transfer rate and a higher overall heat transfer coefficient as expected. In the separate experimental runs, results showed that the frost grew more from the top half of the heat exchanger as time progressed. The amount of frost formation increased as air flow rate decreased. This is because the surface of the heat exchanger becomes colder for a lower flow rate due to a lower heat transfer rate. The trend concerning the effect of air flow rate on frost formation is consistent with the experiments of Senshu et al. [5]. However, it is contradictory to those of Rite and Crawford [9]. A decrease in air flow rate resulted in an increase in the frosting rate, thus the heat transfer rate and the overall heat transfer coefficient degraded faster. As shown in Fig. 1(c), the experimental data indicated that an increased flow rate resulted in a higher pressure drop initially. This is similar to the trends of dry heat exchangers. However, after 80 min the pressure drop for $Q_a = 12$ m^3/min became the largest.

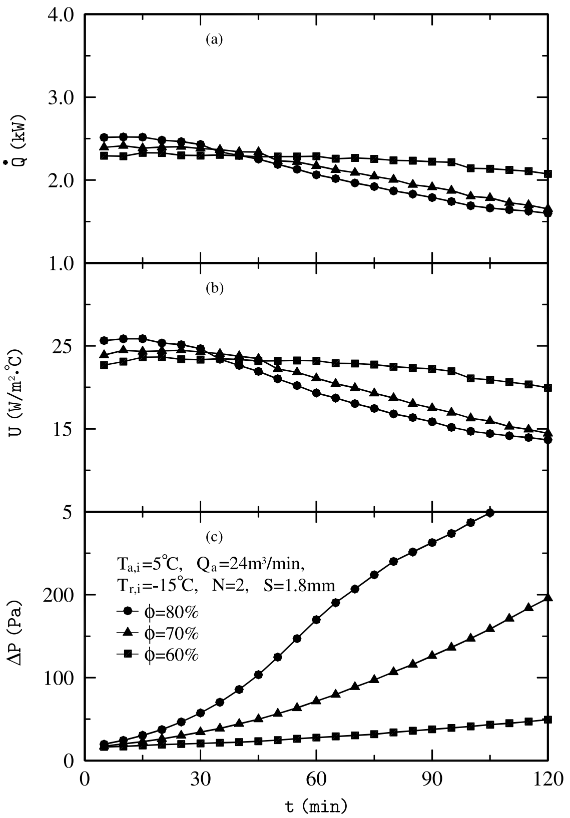

Fig. 2. Effects of air relative humidity on (a) heat transfer rate, (b) overall heat transfer coefficient, and (c) pressure drop.

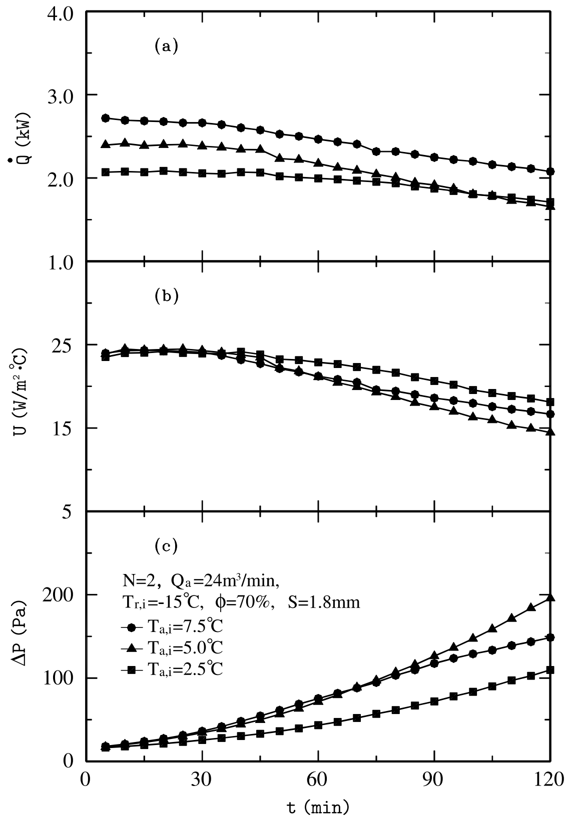

Fig. 3. Effects of air temperature on (a) heat transfer rate, (b) overall heat transfer coefficient, and (c) pressure drop.

This was because there was more frost formation blocking the flow passage and increased the pressure drop.

The effects of the air relative humidity on the performance of the heat exchanger are presented in Fig. 2. Initially, the heat transfer rate and the overall heat transfer coefficient are very close to one another for 60%, 70% and 80% relative humidities. Air with a higher relative humidity has a higher moisture content and leads to more frost formation. As a consequence, the heat transfer rate and the overall heat transfer coefficient drop more quickly for higher relative humidities. The trend of increasing frost formation with humidity is consistent with that reported by Rite and Crawford [9]. Fig. 2(c) shows the effects of the relative humidity on the pressure drop. As the relative humidity increases, there is a higher pressure drop across the heat exchanger.

The effects of air temperature on the heat transfer rate, the overall heat transfer coefficient, and the pressure drop are shown in Fig. 3. A higher air temperature resulted in a higher temperature difference between the air and the refrigerant. In addition, the humidity ratio was higher for a higher air temperature with the same relative humidity. Generally speaking, the heat transfer rate increased as air temperature increased. The surface of the heat exchanger became warmer for a higher air temperature. However, the air contains more moisture. A higher surface temperature is detrimental to the frost formation, but a higher moisture is favorable for the frost growth. From Fig. 3(c), it is interesting to note that there is an increase in the pressure drop when the air temperature was increased from 2.5 to 5 °C. This indicates that the amount of frost increases as the air temperature increases. Thus the effect of the moisture is more important than the effect of the surface temperature on frost accumulation. However, the pressure drop decreased as the air temperature was increased from 5 to 7.5 °C. It means that the amount of frost decreases as air temperature increases. Obviously, the effect of the surface temperature is dominant.

Fig. 4 shows the heat transfer rate, overall heat transfer coefficient, and pressure drop versus time for different refrigerant temperatures. A lower refrigerant temperature leaded to a lower surface temperature of the heat exchanger and a greater amount of frost; therefore, it had a larger heat transfer rate and a higher pressure

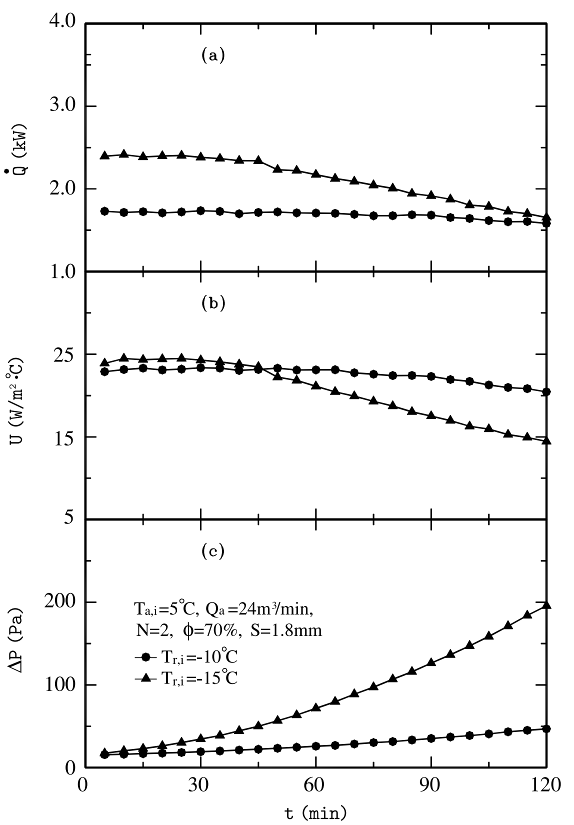

Fig. 4. Effects of refrigerant temperature on (a) heat transfer rate, (b) overall heat transfer coefficient, and (c) pressure drop.

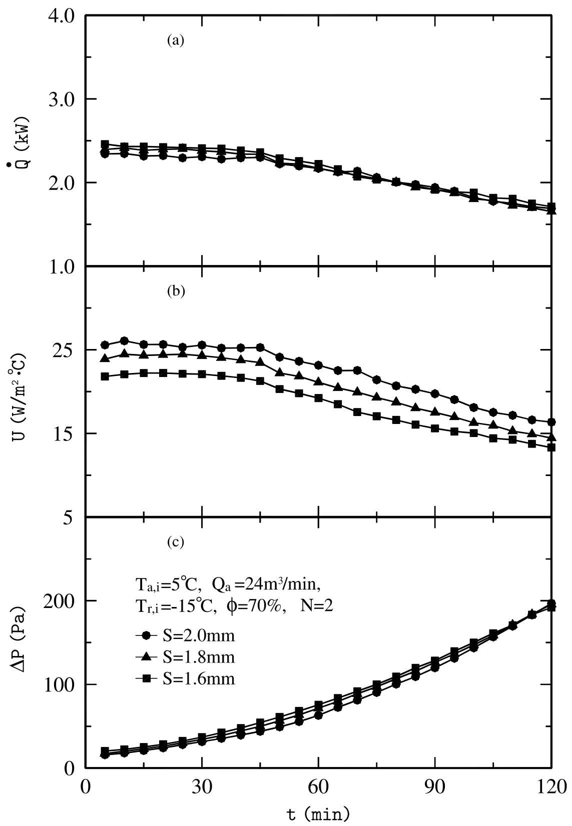

Fig. 5. Effects of fin pitch on (a) heat transfer rate, (b) over all heat transfer coefficient, and (c) pressure drop.

drop. The trends are consistent with the results of Rite and Crawford [9]. It was also noted that for a lower refrigerant temperature, the heat transfer rate declined and the pressure drop increased more rapidly. Because of a higher frost formation, the frost insulates and blocks the heat exchanger more quickly.

Fig. 5 shows the effects of the fin pitch on the performance of the heat exchanger. The heat transfer rate and the pressure drop are very close for different fin pitches. The overall heat transfer coefficient is higher for a heat exchanger with a larger fin pitch. This is a consequence of the decrease of the area.

The effects of the row number on the heat transfer and the pressure drop characteristics are shown in Fig. 6. It is noted from Fig. 6(a) and (b) that a larger row number resulted in a higher heat transfer rate and a lower overall heat transfer coefficient due to the increase of heat transfer area. The air pressure drop across the heat exchanger increased with the row number initially. This is because a heat exchanger with a larger row number is thicker in the flow direction. The surface temperature of the heat exchanger increases with the row number. It is a consequence of the higher heat transfer rate. This results in a decreased frost accumulation. However, the pressure drop of the heat exchanger with one tube row becomes the highest eventually.

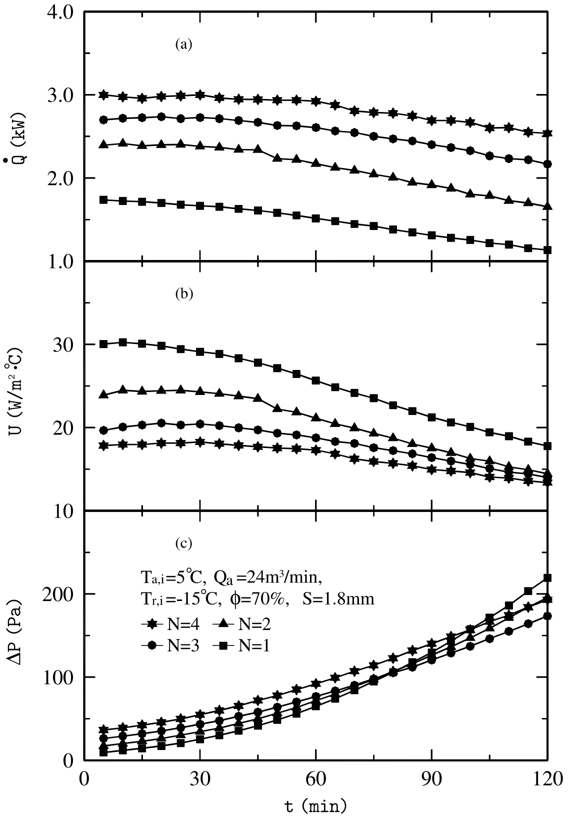

Fig. 6. Effects of row number on (a) heat transfer rate, (b) overall heat transfer coefficient, and (c) pressure drop.

5. Conclusion

The performance of flat plate finned tube heat exchangers under frosting conditions was investigated experimentally. The following conclusions were made:

1. The frost formation is greater for a lower air flow rate, and the rate of pressure drop increases.
2. The rate of pressure drop increases rapidly as the relative humidity increases.
3. The performance of the heat exchanger is not affected significantly by the fin pitch provided the fin spacing is large.

Acknowledgements

The support of this work by the National Science Council of the Republic of China (contract no. NSC 88-2212-E-211-003) and the Industrial Technology Research Institute is gratefully acknowledged.

References

[1] D.H. Niederer, Frosting and defrosting effects on coil heat transfer, ASHRAE Trans. 92 (Part 1) (1986) 467–473.
[2] S.N. Kondepudi, D.L. O'Neal, The effects of frost growth on extended surface heat exchanger performance: A review, ASHRAE Trans. 93 (Part 2) (1987) 258–277.
[3] S.N. Kondepudi, D.L. O'Neal, Effect of frost growth on the performance of louvered finned tube heat exchangers, Int. J. Refrig. 12 (1989) 151–158.
[4] S.N. Kondepudi, D.L. O'Neal, The effects of different fin configurations on the performance of finned-tube heat exchangers under frosting conditions, ASHRAE Trans. 96 (Part 2) (1990) 439–444.
[5] T. Senshu, H. Yasuda, K. Oguni, K. Ishibani, Heat pump performance under frosting condition: Part I—Heat and mass transfer on cross-finned tube heat exchangers under frosting condition, ASHRAE Trans. 96 (Part 1) (1990) 324–329.
[6] H. Yasuda, T. Senshu, S. Kuroda, A. Atsumi, K. Oguni, Heat pump performance under frosting condition: Part II—Simulation of heat pump cycle characteristics under frosting condition, ASHRAE Trans. 96 (Part 1) (1990) 330–336.
[7] S.P. Oskarsson, K.I. Karkow, S. Lin, Evaporator models for operation with dry, wet, and frosted finned surfaces Part I: Heat transfer and fluid flow theory, ASHRAE Trans. 96 (Part 1) (1990) 373–380.
[8] S.P. Oskarsson, K.I. Karkow, S. Lin, Evaporator models for operation with dry, wet, and frosted finned surfaces

Part II: Evaporator models and verification, ASHRAE Trans. 96 (Part 1) (1990) 381–392.
[9] R.W. Rite, R.R. Crawford, The effect of frost accumulation on the performance of domestic refrigerator-freezer finned-tube evaporator coils, ASHRAE Trans. 97 (Part 2) (1991) 428–437.
[10] R.W. Rite, R.R. Crawford, A parametric study of the factors governing the rate of frost accumulation on domestic refrigerator-freezer finned-tube evaporator coils, ASHRAE Trans. 97 (Part 2) (1991) 438–446.
[11] S.N. Kondepudi, D.L. O'Neal, Performance of finned-tube heat exchangers under frosting conditions: I. simulation model, Int. J. Refrig. 16 (3) (1993) 175–180.
[12] S.N. Kondepudi, D.L. O'Neal, Performance of finned-tube heat exchangers under frosting conditions: II. comparison of experimental data with model, Int. J. Refrig. 16 (3) (1993) 181–184.
[13] L. Thomas, H. Chen, R.W. Besant, Measurement of frost characteristics on heat exchanger fins Part I: Test facility and instrumentation, ASHRAE Trans. 105 (Part 2) (1999) 283–293.
[14] H. Chen, L. Thomas, R.W. Besant, Measurement of frost characteristics on heat exchanger fins Part II: Data and analysis, ASHRAE Trans. 105 (Part 2) (1999) 294–298.
[15] ASHRAE Standard 41.1-1986, 1986, Standard Method for Temperature Measurement, American Society of Heating, Refrigerating, and Air-Conditioning Engineers, Atlanta, GA.
[16] ASHRAE Standard 41.2-1987, 1987, Standard Methods for Laboratory Air-flow Measurement, American Society of Heating, Refrigerating, and Air-Conditioning Engineers, Atlanta, GA.
[17] S.T. Kline, F.A. McClintock, Describing uncertainties in single-sample experiments, Mech. Eng. 75 (1953) 3–8.